

SUPPORTING INFORMATION

Quantification of Membrane Protein-Detergent Complex Interactions

Aaron J. Wolfe,^{1,2} Wei Si,^{3,4} Zhengqi Zhang,⁵ Adam R. Blanden,⁶ Yi-Ching Hsueh,¹ Jack F. Gugel,¹ Bach Pham,⁷ Min Chen,⁷ Stewart N. Loh,⁶ Sharon Rozovsky,⁵ Aleksei Aksimentiev,^{*4} and Liviu Movileanu^{*1,2,8}

¹*Department of Physics, Syracuse University, 201 Physics Building, Syracuse, New York 13244-1130, USA*

²*Structural Biology, Biochemistry, and Biophysics Program, Syracuse University, 111 College Place, Syracuse, New York 13244-4100, USA*

³*Jiangsu Key Laboratory for Design and Manufacture of Micro-Nano Biomedical Instruments and School of Mechanical Engineering, Southeast University, Nanjing, 210096, China*

⁴*Department of Physics, University of Illinois at Urbana-Champaign, Urbana, Illinois 61801, USA*

⁵*Department of Chemistry and Biochemistry, University of Delaware, 136 Brown Laboratory, Newark, Delaware 19716, USA*

⁶*Department of Biochemistry and Molecular Biology, State University of New York Upstate Medical University, 4249 Weiskotten Hall, 766 Irving Av., Syracuse, New York 13210, USA*

⁷*Department of Chemistry, University of Massachusetts, 820 LGRT, 710 North Pleasant Street, Amherst, Massachusetts 01003-9336, USA*

⁸*Department of Biomedical and Chemical Engineering, Syracuse University, 329 Link Hall, Syracuse, New York 13244, USA*

Running title: Quantification of protein-detergent complex interactions

Correspondence/materials requests:

*Liviu Movileanu, PhD, Department of Physics, Syracuse University, 201 Physics Building, Syracuse, New York 13244-1130, USA; Phone: 315-443-8078; Fax: 315-443-9103; E-mail: lmovilea@syr.edu; aksiment@illinois.edu

1. Characterization of SELENOK U92C and SELENOS U188S proteins prior to and following labeling with Texas Red

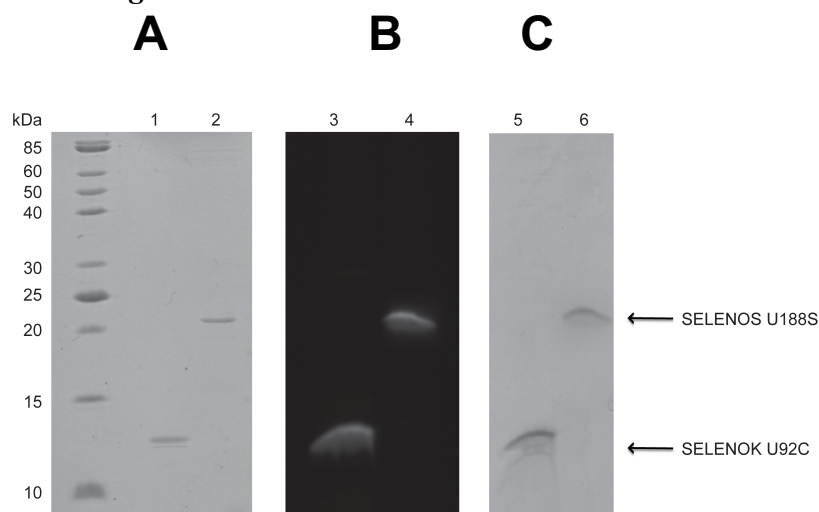


Figure S1: Characterization of SELENOK U92C and SELENOS U188S prior to and following labeling with Texas Red. (A) The purity of SELENOK U92C (lane 1) and SELENOS U188S (lane 2) prior to labeling was assessed from 16% Tris-Glycine SDS-PAGE. Electrophoresis was performed under reducing conditions. The molecular weights of SELENOK U92C and SELENOS U188S are 11.5 and 21.2 kDa, respectively. (B) The fluorescence of SELENOS U188S and SELENOK U92C labeled with Texas Red C2-maleimide was visualized using a FluorChem Q imaging system (Alpha Innotech, San Jose, CA) with a Cy5 filter (lanes 3 and 4). (C) The same gel from B was visualized by coomassie-blue staining (lanes 5 and 6).

2. Example of steady-state FP traces illustrating no time-dependent alterations in the anisotropy readout at detergent concentrations much greater than their corresponding CMCs

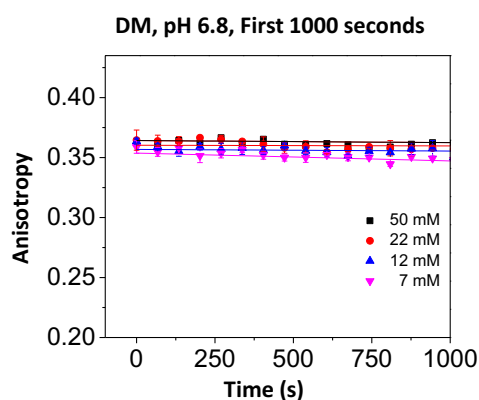


Figure S2: Time-dependent fluorescence anisotropy traces acquired with n-Decyl- β -D-maltoside (DM). The anisotropy data were collected by adding overnight refolded protein to a bath of varying detergent concentration, as indicated in the legend. All anisotropy measurements were conducted at room temperature in 200 mM NaCl, 50 mM HEPES, pH 6.8. Time-dependent anisotropy measurements were executed directly after dilution of the refolded protein sample at respective detergent concentration. Final protein concentration was maintained at 28 nM.

3. Example of steady-state FP traces showing no time-dependent alterations in the anisotropy readout after 24 hours, regardless of the detergent concentration inspected in this work.

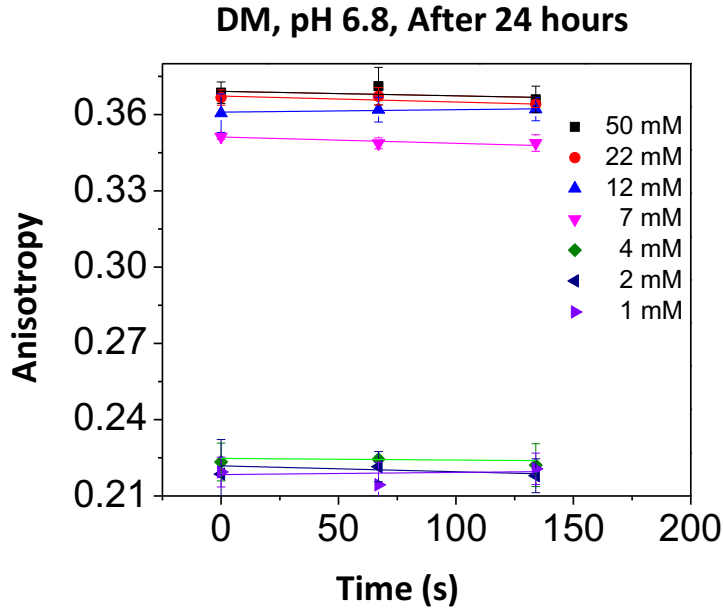


Figure S3: Anisotropy readout was collected after 24 hours, but under similar experimental conditions with those mentioned in the caption of Fig. S2.

4. **Hydrodynamic changes of the proteomicelles during the transition of detergent desolvation.** Data resulting from steady-state FP measurements were used to derive the hydrodynamic radius of the proteins under detergent solvation and desolvation conditions. Perrin's equation relates the rotational diffusion coefficient, D_r , to the steady-state fluorescence anisotropy, r ,¹

$$\frac{r_0}{r} = 1 + 6D_r \tau_F \quad (\text{S1})$$

r_0 indicates the fundamental maximum anisotropy value. Here, τ_F is the fluorescence lifetime of the fluorophore. In the case of Texas Red, r_0 is 0.4,² whereas τ_F is 4.2 ns.³ The rotational correlation time, θ , relates to the apparent hydrodynamic volume of the labeled molecule, V_h , as follows:³

$$\theta = \frac{1}{6D_r} \quad (\text{S2})$$

$$V_h = \frac{\theta k_B T}{\eta} = \frac{k_B T}{6\eta D_r} \quad (\text{S3})$$

Using (S1) and (S2):

$$\frac{r_0}{r} = 1 + \frac{\tau_F}{\theta} \quad (\text{S4})$$

Here, the dynamic viscosity of the buffer solution that corresponds to 200 mM NaCl, η , is 1.028 mPa s.⁴ k_B and T denote the Boltzmann constant and absolute temperature, respectively. Therefore, we determined the rotational diffusion coefficients of the fully solvated proteins, D_r^{slow} , and detergent-desolvated proteins, D_r^{fast} , as well as the average maximum hydrodynamic radii, R_h^{max} (**Table3**).

Table S1: Table that summarizes the recorded minima and maxima of the anisotropy readout with neutral, maltoside-containing detergents and the four β -barrel proteins.^a This table also illustrates the rotational diffusion coefficients as well as alterations in hydrodynamic radii of the proteomicelles during the detergent desolvation transitions.

DDM ^b	r_{\min}^c	r_{\max}^c	$D_r^{\text{slow}} (10^7 \text{ s}^{-1})^d$	$D_r^{\text{fast}} (10^7 \text{ s}^{-1})^d$	$R_h^{\text{max}} (\text{nm})^e$	$\Delta R_h (\text{nm})^f$
OmpG	ND ^g	0.330 ± 0.004	0.84 ± 0.06	ND ^g	2.7	ND ^g
FhuA $\Delta C/\Delta 5L$	0.196 ± 0.054	0.336 ± 0.003	0.76 ± 0.04	4.1 ± 1.7	2.8	1.2 ± 0.2
FhuA $\Delta C/\Delta 5L_{25N}$	0.181 ± 0.008	0.315 ± 0.003	1.1 ± 0.1	4.8 ± 0.4	2.5	0.97 ± 0.07
FhuA $\Delta C/\Delta 7L_{30N}$	0.183 ± 0.012	0.314 ± 0.002	1.1 ± 0.1	4.7 ± 0.5	2.5	0.95 ± 0.08
UM ^b	r_{\min}^c	r_{\max}^c	$D_r^{\text{slow}} (10^7 \text{ s}^{-1})^d$	$D_r^{\text{fast}} (10^7 \text{ s}^{-1})^d$	$R_h^{\text{max}} (\text{nm})^e$	$\Delta R_h (\text{nm})^f$
OmpG	0.216 ± 0.006	0.319 ± 0.002	1.1 ± 0.1	3.4 ± 0.2	2.5	0.83 ± 0.06
FhuA $\Delta C/\Delta 5L$	0.230 ± 0.015	0.357 ± 0.003	0.48 ± 0.04	2.9 ± 0.4	3.2	1.5 ± 0.2
FhuA $\Delta C/\Delta 5L_{25N}$	0.186 ± 0.002	0.322 ± 0.002	0.96 ± 0.03	4.6 ± 0.01	2.6	1.0 ± 0.1
FhuA $\Delta C/\Delta 7L_{30N}$	0.208 ± 0.005	0.312 ± 0.002	1.1 ± 0.1	3.7 ± 0.2	2.4	0.79 ± 0.05
DM ^b	r_{\min}^c	r_{\max}^c	$D_r^{\text{slow}} (10^7 \text{ s}^{-1})^d$	$D_r^{\text{fast}} (10^7 \text{ s}^{-1})^d$	$R_h^{\text{max}} (\text{nm})^e$	$\Delta R_h (\text{nm})^f$
OmpG	0.214 ± 0.005	0.327 ± 0.001	0.89 ± 0.02	3.5 ± 0.2	2.6	0.95 ± 0.04
FhuA $\Delta C/\Delta 5L$	0.219 ± 0.005	0.360 ± 0.001	0.44 ± 0.01	3.3 ± 0.2	3.3	1.6 ± 0.1
FhuA $\Delta C/\Delta 5L_{25N}$	0.166 ± 0.003	0.343 ± 0.002	0.66 ± 0.03	5.6 ± 0.2	3.0	1.5 ± 0.1
FhuA $\Delta C/\Delta 7L_{30N}$	0.168 ± 0.007	0.312 ± 0.001	1.1 ± 0.1	5.5 ± 0.4	2.4	1.0 ± 0.1
CYMAL-4 ^b	r_{\min}^c	r_{\max}^c	$D_r^{\text{slow}} (10^7 \text{ s}^{-1})^d$	$D_r^{\text{fast}} (10^7 \text{ s}^{-1})^d$	$R_h^{\text{max}} (\text{nm})^e$	$\Delta R_h (\text{nm})^f$
OmpG	0.163 ± 0.001	0.326 ± 0.001	0.90 ± 0.01	5.8 ± 0.1	2.6	1.2 ± 0.1
FhuA $\Delta C/\Delta 5L$	0.242 ± 0.001	0.367 ± 0.001	0.36 ± 0.01	2.6 ± 0.1	3.6	1.7 ± 0.1
FhuA $\Delta C/\Delta 5L_{25N}$	0.166 ± 0.001	0.341 ± 0.001	0.69 ± 0.01	5.6 ± 0.2	2.9	1.4 ± 0.1
FhuA $\Delta C/\Delta 7L_{30N}$	0.168 ± 0.025	0.345 ± 0.004	0.63 ± 0.05	5.5 ± 1.2	2.9	1.5 ± 0.2

^aTo reach low detergent concentrations below CMC, the Gdm-HCl-solubilized proteins were refolded at various detergent concentrations above CMC.

^bFull names of the detergents are provided in **Experimental Methods**.

^cExperimentally determined anisotropy minima (r_{\min}) and maxima (r_{\max}) for various detergents. r_{\min} was extrapolated for the lowest detergent concentration in the well. r_{\max} was determined for detergent concentrations above the CMC.

^d D_r^{slow} and D_r^{fast} indicate the rotational diffusion coefficients of the protein under solvation and desolvation conditions, respectively.

^e R_h^{max} are the maximum hydrodynamic radii of the proteomicelle with various solubilizing detergents.

^f ΔR_h is the decrease in the hydrodynamic radius, R_h , as a result of the detergent desolvation transition of the protein.

^gNot determined.

Table S2: Summary of the fitting results of the two-state, concentration-dependent anisotropy curves acquired with neutral, maltoside-containing detergents.^{a,b} This was determined with three FhuA derivatives and OmpG as well as a panel of five neutral detergents of varying hydrophobic chain and hydrophilic head group. The FP measurements were carried in 200 mM NaCl, 50 mM HEPES, pH 7.4 and at a temperature of 24°C. All data were derived as averages \pm SDs of three independent data acquisitions.

DDM ^c	p^d	K_d^e (mM)	q^f (mM ⁻¹)	ΔG^g (kcal/mol)	Balance ^h
OmpG	1.4 \pm 0.9	~0.11	0.99	-5.4 \pm 1.2	$F_{adh} \gg F_{coh}$
FhuA $\Delta C/\Delta 5L$	1.1 \pm 0.3	0.52 \pm 0.36	0.07	-4.5 \pm 0.7	$F_{adh} \leq F_{coh}$
FhuA $\Delta C/\Delta 5L_{25N}$	4.4 \pm 2.8	0.62 \pm 0.17	0.24	-4.4 \pm 0.1	$F_{adh} < F_{coh}$
FhuA $\Delta C/\Delta 7L_{30N}$	4.4 \pm 1.6	0.64 \pm 0.10	0.22	-4.3 \pm 0.1	$F_{adh} < F_{coh}$
UM ^c	p^d	K_d^e (mM)	q^f (mM ⁻¹)	ΔG^g (kcal/mol)	Balance ^h
OmpG	4.8 \pm 3.1	0.49 \pm 0.17	0.25	-4.5 \pm 0.3	$F_{adh} \leq F_{coh}$
FhuA $\Delta C/\Delta 5L$	3.5 \pm 0.9	0.29 \pm 0.05	0.38	-4.8 \pm 0.1	$F_{adh} > F_{coh}$
FhuA $\Delta C/\Delta 5L_{25N}$	4.9 \pm 0.3	0.59 \pm 0.02	0.28	-4.4 \pm 0.1	$F_{adh} \cong F_{coh}$
FhuA $\Delta C/\Delta 7L_{30N}$	4.6 \pm 1.1	0.69 \pm 0.07	0.17	-4.3 \pm 0.1	$F_{adh} \cong F_{coh}$
DM ^c	p^d	K_d^e (mM)	q^f (mM ⁻¹)	ΔG^g (kcal/mol)	Balance ^h
OmpG	4.1 \pm 1.2	1.8 \pm 0.4	0.064	-3.7 \pm 0.1	$F_{adh} \cong F_{coh}$
FhuA $\Delta C/\Delta 5L$	3.5 \pm 0.5	1.7 \pm 0.1	0.072	-3.8 \pm 0.1	$F_{adh} \cong F_{coh}$
FhuA $\Delta C/\Delta 5L_{25N}$	27 \pm 3	0.9 \pm 0.1	1.30	-4.1 \pm 0.1	$F_{adh} \gg F_{coh}$
FhuA $\Delta C/\Delta 7L_{30N}$	27 \pm 6	0.9 \pm 0.1	1.07	-4.1 \pm 0.1	$F_{adh} \gg F_{coh}$
CYMAL-4 ^c	p^d	K_d^e (mM)	q^f (mM ⁻¹)	ΔG^g (kcal/mol)	Balance ^h
OmpG	6.7 \pm 0.1	4.6 \pm 0.1	0.25	-3.2 \pm 0.1	$F_{adh} > F_{coh}$
FhuA $\Delta C/\Delta 5L$	3.7 \pm 0.1	5.3 \pm 0.1	0.38	-3.1 \pm 0.1	$F_{adh} > F_{coh}$
FhuA $\Delta C/\Delta 5L_{25N}$	5.2 \pm 0.3	5.7 \pm 0.1	0.28	-3.1 \pm 0.1	$F_{adh} > F_{coh}$
FhuA $\Delta C/\Delta 7L_{30N}$	2.3 \pm 0.9	4.5 \pm 1.1	0.17	-3.2 \pm 0.1	$F_{adh} > F_{coh}$

^aTo reach low detergent concentrations below the CMC, the Gdm-HCl-solubilized proteins were refolded at detergent concentrations above the CMC.

^bThe dose-response equilibrium curves were fitted by the four-parameter Hill equation (eq. (3)).

^cThis column indicates the names of the detergents and proteins used in this work. Other details are provided in **Methods**.

^d p is the Hill coefficient.

^eThe apparent dissociation constant, K_d , was determined as the midpoint of the dose-dependent dissociation phase (e.g., c_0).⁵

^fThe slope factor or transition steepness was calculated at the midpoint of the dissociation phase.

^gFree energies were determined using the standard thermodynamic relationship $\Delta G = RT \ln K_d$.

^hThe semi-quantitative balance between the adhesive protein-detergent (F_{adh}) and cohesive detergent-detergent interactions (F_{coh}) of the proteomicelles.

5. Time-dependent changes in the FP anisotropy when the four β -barrel proteins were incubated in CHAPS at detergent concentrations above and below the CMC

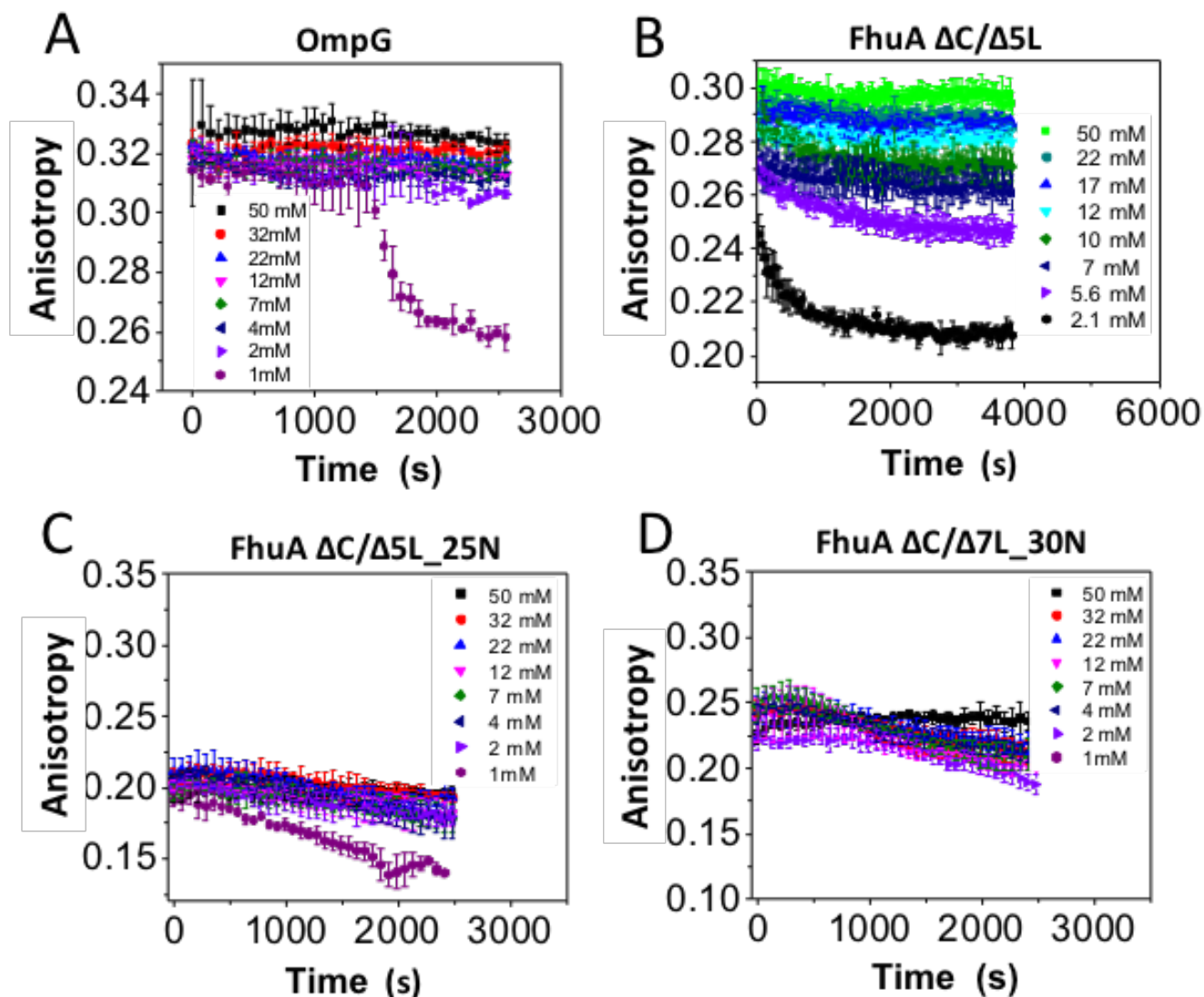


Figure S4: Time-dependent changes in the FP anisotropy when the four β -barrel proteins were incubated in CHAPS at detergent concentrations above and below the CMC. (A) OmpG; (B) FhuA $\Delta C/\Delta 5L$; (C) FhuA $\Delta C/\Delta 5L_{25N}$; (D) FhuA $\Delta C/\Delta 7L_{30N}$. The other experimental conditions were similar to those presented in Fig. 3 and Table 4.

6. Time-dependent changes in the FP anisotropy when the four β -barrel proteins were incubated in LD.

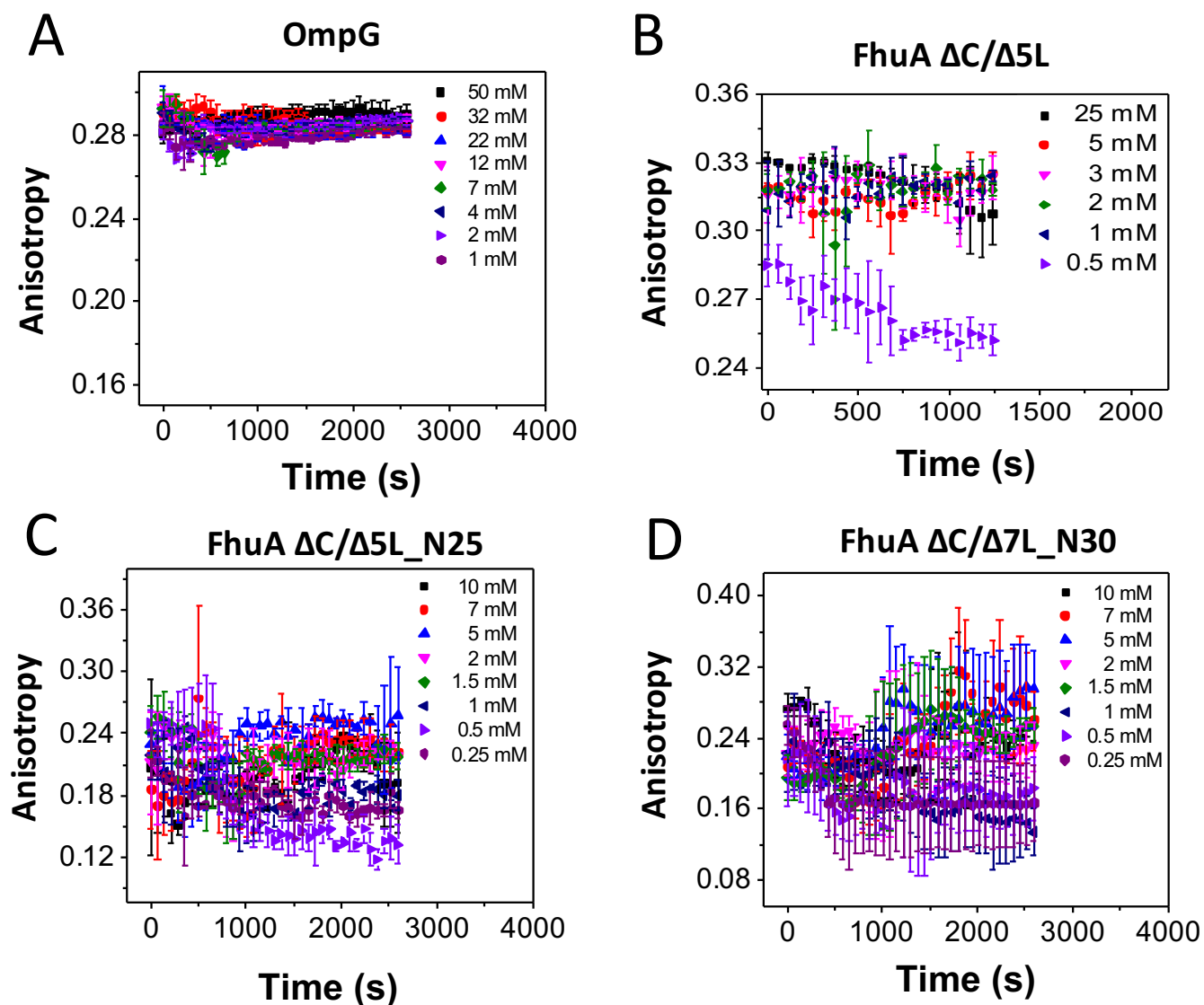


Figure S5: Time-dependent changes in the FP anisotropy when the four β -barrel proteins were incubated in n-dodecyl-N,N-dimethylglycine (LD). (A) OmpG; (B) FhuA Δ C/ Δ 5L; (C) FhuA Δ C/ Δ 5L_25N; (D) FhuA Δ C/ Δ 7L_30N. The other experimental conditions were similar to those presented in Fig. 3 and Table 4.

Table S3: Table that summarizes the recorded minima and maxima of the anisotropy readout with DM and the four β -barrel proteins under conditions of varying pH.^a This table also illustrates the rotational diffusion coefficients as well as alterations in the hydrodynamic radii of the proteomicelles during the two-state detergent desolvation transitions.

OmpG ^b	r_{\min}^c	r_{\max}^c	$D_r^{\text{slow}} (10^7 \text{ s}^{-1})^d$	$D_r^{\text{fast}} (10^7 \text{ s}^{-1})^d$	$R_h^{\text{max}} (\text{nm})^e$	$\Delta R_h (\text{nm})^f$
4.6	0.094 ± 0.004	0.219 ± 0.005	3.3 ± 0.2	13 ± 1	1.7	0.62 ± 0.05
5.6	0.112 ± 0.009	0.303 ± 0.001	1.3 ± 0.1	10 ± 1	2.3	1.2 ± 0.1
6.8	0.151 ± 0.019	0.331 ± 0.002	0.83 ± 0.02	6.5 ± 1.2	2.7	1.3 ± 0.1
7.4	0.214 ± 0.005	0.327 ± 0.001	0.89 ± 0.02	3.4 ± 0.2	2.6	0.95 ± 0.04
8.2	0.150 ± 0.027	0.334 ± 0.001	0.79 ± 0.01	6.6 ± 1.6	2.7	1.4 ± 0.1
10	0.169 ± 0.004	0.337 ± 0.001	0.74 ± 0.01	5.4 ± 0.2	2.8	1.3 ± 0.1
FhuA $\Delta C/\Delta 5L^b$	r_{\min}^c	r_{\max}^c	$D_r^{\text{slow}} (10^7 \text{ s}^{-1})^d$	$D_r^{\text{fast}} (10^7 \text{ s}^{-1})^d$	$R_h^{\text{max}} (\text{nm})^e$	$\Delta R_h (\text{nm})^f$
4.6	0.161 ± 0.005	0.235 ± 0.003	2.8 ± 0.1	5.8 ± 0.2	1.8	0.40 ± 0.04
5.6	0.195 ± 0.016	0.365 ± 0.002	0.38 ± 0.02	4.2 ± 0.6	3.5	1.9 ± 0.1
6.8	0.216 ± 0.005	0.366 ± 0.002	0.37 ± 0.02	3.4 ± 0.2	3.5	1.8 ± 0.1
7.4	0.219 ± 0.005	0.360 ± 0.001	0.44 ± 0.01	3.3 ± 0.2	3.3	1.6 ± 0.1
8.2	0.117 ± 0.024	0.373 ± 0.002	0.29 ± 0.02	9.6 ± 2.3	3.8	2.6 ± 0.2
10	~0.238	0.329 ± 0.003	~0.86	~2.7	2.6	~0.84
FhuA $\Delta C/\Delta 5L_25N^b$	r_{\min}^c	r_{\max}^c	$D_r^{\text{slow}} (10^7 \text{ s}^{-1})^d$	$D_r^{\text{fast}} (10^7 \text{ s}^{-1})^d$	$R_h^{\text{max}} (\text{nm})^e$	$\Delta R_h (\text{nm})^f$
4.6	0.176 ± 0.024	0.307 ± 0.002	1.2 ± 0.3	5.1 ± 1.1	2.4	0.89 ± 0.11
5.6	0.154 ± 0.002	0.326 ± 0.001	0.90 ± 0.01	6.3 ± 0.1	2.6	1.2 ± 0.1
6.8	0.144 ± 0.009	0.327 ± 0.005	0.89 ± 0.07	7.1 ± 0.7	2.6	1.3 ± 0.1
7.4	0.166 ± 0.003	0.343 ± 0.002	0.66 ± 0.03	5.6 ± 0.2	2.9	1.5 ± 0.1
8.2	0.168 ± 0.004	0.309 ± 0.001	1.2 ± 0.02	5.5 ± 0.2	2.4	0.96 ± 0.02
10	ND ^g	0.265 ± 0.007	2.0 ± 0.2	ND ^g	2.0	ND ^g
FhuA $\Delta C/\Delta 7L_30N^b$	r_{\min}^c	r_{\max}^c	$D_r^{\text{slow}} (10^7 \text{ s}^{-1})^d$	$D_r^{\text{fast}} (10^7 \text{ s}^{-1})^d$	$R_h^{\text{max}} (\text{nm})^e$	$\Delta R_h (\text{nm})^f$
4.6	0.198 ± 0.006	0.348 ± 0.001	0.59 ± 0.01	4.1 ± 0.2	3.0	1.4 ± 0.1
5.6	0.178 ± 0.010	0.338 ± 0.002	0.73 ± 0.03	5.0 ± 0.5	2.8	1.3 ± 0.1
6.8	0.155 ± 0.016	0.296 ± 0.006	1.4 ± 0.1	6.3 ± 1.0	2.3	0.89 ± 0.12
7.4	0.168 ± 0.007	0.312 ± 0.001	1.1 ± 0.1	5.5 ± 0.4	2.4	1.0 ± 0.1
8.2	0.151 ± 0.010	0.284 ± 0.026	1.6 ± 0.5	6.5 ± 0.7	2.1	0.80 ± 0.22
10	0.325 ± 0.009	0.358 ± 0.001	0.4 ± 0.1	0.9 ± 0.1	3.2	0.66 ± 0.14

^aTo reach low detergent concentrations below CMC, the Gdm-HCl-solubilized FhuA $\Delta C/\Delta 5L$ protein was refolded at various detergent concentrations above CMC. These values were stated in **Methods**.

^bFull names of the detergents are provided in **Methods**.

^cExperimentally determined anisotropy minima (r_{\min}) and maxima (r_{\max}) for various detergents. r_{\min} was extrapolated for the lowest detergent concentration in the well. r_{\max} was determined for detergent concentrations above the CMC.

^d D_r^{slow} and D_r^{fast} indicate the rotational diffusion coefficients of the FhuA $\Delta C/\Delta 5L$ protein under solvation and desolvation conditions, respectively.

^e R_h^{max} are the maximum hydrodynamic radii of the proteomicelle with various solubilizing detergents.

^f ΔR_h is the decrease in the hydrodynamic radius, R_h , as a result of the detergent desolvation transition of the protein.

ND^g Not determined.

Table S4: Summary of the fitting results of the two-state, concentration-dependent anisotropy curves acquired with three FhuA derivatives and OmpG under conditions of varying pH.^{a,b} DM was the detergent used in this case. The solution contained 200 mM NaCl at room temperature. The buffer was either 50 mM HEPES (pH 6.8, pH 7.4, pH 8.2), 50 mM NaOAc (pH 4.6, pH 5.6) or 50 mM Sodium borate (pH 10.0). All data were derived as averages \pm SDs of three independent data acquisitions.

OmpG ^c	p^d	K_d^e (mM)	q^f (mM ⁻¹)	ΔG^g (kcal/mol)	Balance ^h
4.6	3.7 \pm 1.2	1.6 \pm 0.5	0.05	-3.8 \pm 0.2	$F_{adh} \cong F_{coh}$
5.6	6.5 \pm 6.8	1.8 \pm 0.6	0.17	-3.7 \pm 0.2	$F_{adh} \cong F_{coh}$
6.8	6.2 \pm 3.4	1.5 \pm 0.4	0.18	-3.8 \pm 0.2	$F_{adh} \cong F_{coh}$
7.4	4.1 \pm 1.2	1.8 \pm 0.4	0.064	-3.7 \pm 0.1	$F_{adh} \cong F_{coh}$
8.2	5.2 \pm 2.1	1.5 \pm 0.4	0.17	-3.9 \pm 0.2	$F_{adh} \cong F_{coh}$
10	3.6 \pm 0.2	1.3 \pm 0.1	0.12	-3.9 \pm 0.1	$F_{adh} > F_{coh}$
FhuA $\Delta C/\Delta 5L^c$	p^d	K_d^e (mM)	q^f (mM ⁻¹)	ΔG^g (kcal/mol)	Balance ^h
4.6	~25	~2.1	0.23	~-3.6	$F_{adh} < F_{coh}$
5.6	3.7 \pm 0.8	1.6 \pm 0.2	0.098	-3.8 \pm 0.1	$F_{adh} \cong F_{coh}$
6.8	5.3 \pm 1.0	1.7 \pm 0.1	0.12	-3.8 \pm 0.1	$F_{adh} \cong F_{coh}$
7.4	3.5 \pm 0.5	1.7 \pm 0.1	0.072	-3.8 \pm 0.1	$F_{adh} \cong F_{coh}$
8.2	1.9 \pm 0.3	0.9 \pm 0.1	0.13	-4.1 \pm 0.1	$F_{adh} > F_{coh}$
10	~2.4	~1.9	0.029	~-3.7	$F_{adh} \cong F_{coh}$
FhuA $\Delta C/\Delta 5L_{25N}^c$	p^d	K_d^e (mM)	q^f (mM ⁻¹)	ΔG^g (kcal/mol)	Balance ^h
4.6	2.9 \pm 0.9	1.9 \pm 0.5	0.049	-3.7 \pm 0.2	$F_{adh} \cong F_{coh}$
5.6	4.5 \pm 0.3	2.0 \pm 0.1	0.10	-3.7 \pm 0.2	$F_{adh} < F_{coh}$
6.8	2.6 \pm 0.6	2.7 \pm 0.5	0.043	-3.5 \pm 0.1	$F_{adh} < F_{coh}$
7.4	27 \pm 2.9	0.9 \pm 0.1	1.30	-4.1 \pm 0.1	$F_{adh} \gg F_{coh}$
8.2	~9.7	1.7 \pm 1.2	0.20	-3.8 \pm 0.7	$F_{adh} \cong F_{coh}$
10	2.0 \pm 6.7	< 2.0	ND ^a	~-5.6	$F_{adh} \cong F_{coh}$
FhuA $\Delta C/\Delta 7L_{30N}^c$	p^d	K_d^e (mM)	q^f (mM ⁻¹)	ΔG^g (kcal/mol)	Balance ^h
4.6	9.0 \pm 7.6	2.0 \pm 0.1	0.17	-3.7 \pm 0.1	$F_{adh} < F_{coh}$
5.6	5.3 \pm 2.7	1.8 \pm 0.3	0.12	-3.7 \pm 0.1	$F_{adh} \cong F_{coh}$
6.8	2.4 \pm 0.9	1.8 \pm 0.4	0.048	-3.7 \pm 0.1	$F_{adh} \cong F_{coh}$
7.4	27 \pm 6	0.9 \pm 0.1	1.07	-4.1 \pm 0.1	$F_{adh} \gg F_{coh}$
8.2	1.3 \pm 0.5	3.2 \pm 1.5	0.014	-3.4 \pm 0.5	$F_{adh} < F_{coh}$
10	5.6 \pm 7.4	3.9 \pm 1.2	0.012	-3.3 \pm 0.2	$F_{adh} < F_{coh}$

^aTo reach low detergent concentrations below the CMC, the Gdm-HCl-solubilized proteins were refolded at detergent concentrations above the CMC. These values were stated in **Methods**.

^bThe dose-response equilibrium curves were fitted by the four-parameter Hill equation.

^cThis column indicates the names of the proteins and various pH values examined used in this work. Other details are provided in **Methods**.

^d p is the Hill coefficient.

^eThe apparent dissociation constant, K_d , was determined as the midpoint of the dose-dependent dissociation phase (e.g., c_0).⁵

^fThe slope factor or transition steepness was calculated at the midpoint of the dissociation phase.

^gFree energies were determined using the standard thermodynamic relationship $\Delta G = RT \ln K_d$.

^hThe semi-quantitative balance between the adhesive protein-detergent (F_{adh}) and cohesive detergent-detergent interactions (F_{coh}) of the proteomicelles.

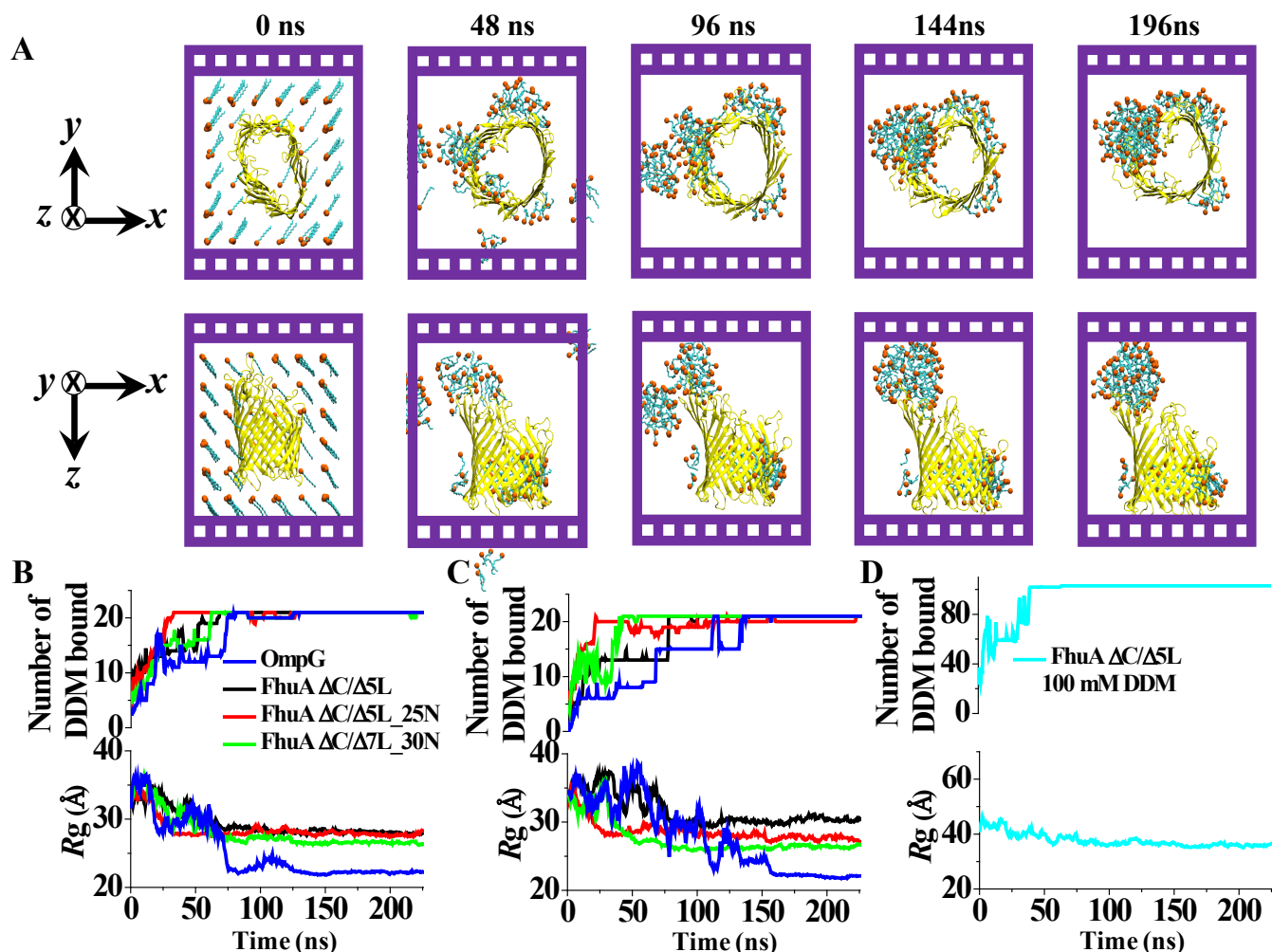


Figure S6: MD simulations of DDM molecules binding to β -barrel proteins. (A) A sequence of microscopic configurations realized in simulations of FhuA $\Delta C/\Delta 5L$ with 100 mM DDM molecules around it. Images in the top and bottom rows depict the same system from two different viewpoints: top view (above) and side view (bottom); (B) The number of the DDM molecules bound to each of the four β -barrel proteins (top) and the radius of gyration of the protein-DDM complex (bottom) versus simulation time. The initial concentration of DDM was 20 mM; the DDM molecules were initially arranged on a cubic lattice around the proteins. The mean values of the R_g for the protein-DDM complexes during the last ~ 70 ns equilibrated simulations are: 22.2 Å for OmpG, 28.1 Å for FhuA $\Delta C/\Delta 5L$, 27.8 Å for FhuA $\Delta C/\Delta 5L_{25N}$ and 26.6 Å for FhuA $\Delta C/\Delta 7L_{30N}$. Each data point represents a 0.48 ns block average of 2.4 ps sampled values; (C) The same as in panel B, but for the initially planar arrangement of the DDM molecules around the proteins. The mean values of the R_g for the protein-DDM complexes during the last ~ 70 ns equilibrated simulations are: 22.1 Å for OmpG, 30.3 Å for FhuA $\Delta C/\Delta 5L$, 27.7 Å for FhuA $\Delta C/\Delta 5L_{25N}$ and 26.4 Å for FhuA $\Delta C/\Delta 7L_{30N}$; (D) The same as in panel B, but for 100 mM DDM concentration. The mean values of the R_g for the protein-DDM complexes during the last ~ 70 ns equilibrated simulation is 35.8 Å.

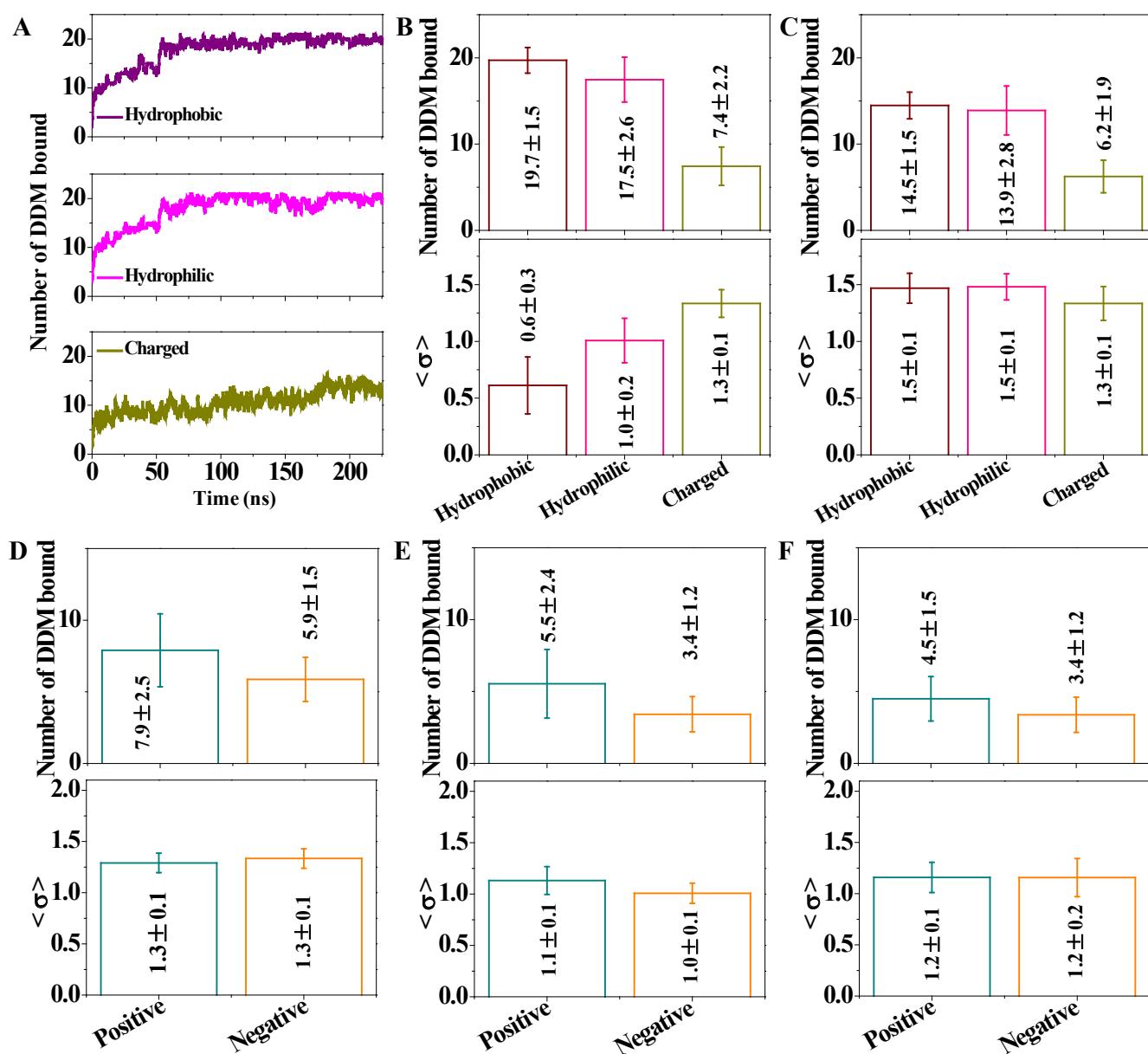


Figure S7: Differential affinity of DDM molecules to residues of β -barrel proteins. (A) The number of DDM molecules bound to the hydrophobic (top), hydrophilic (middle) and charged (bottom) residues of FhuA $\Delta C/\Delta 5L$ versus simulation time. The simulation system contained 20 mM DDM initially placed on a cubic lattice around the protein. The traces were sampled at 2.4 ps intervals and block-averaged in 0.12 ns blocks; (B-C) The mean equilibrium number (top) and the standard deviation (bottom) of the number of DDM molecules bound, with either their tail (panel B) and head (panel C) parts, to the hydrophobic, hydrophilic or charged residues of the four β -barrel proteins. To count as a binding event, any atom of the tail (or the head) part of the molecule must reside within 4 Å of any atom of the hydrophobic, hydrophilic or charged residue of the protein. To compute the mean equilibrium number of bound molecules and its standard deviation, the last ~70 ns of an equilibration trajectory was split into 10 ns fragments; the mean and the standard deviation was computed for each of the fragment and then averaged over all fragments. The final plotted values were obtained by averaging over the two independent MD simulations of each protein system and then over the four protein systems. Error bars

represent standard deviations among the eight simulations; (D-F) Same as in panel B and C but for binding of the entire DDM molecules (panel D), and separately of their tail (panel E) and head (panel F) parts to all positively or negatively charged residues of the β -barrel proteins.

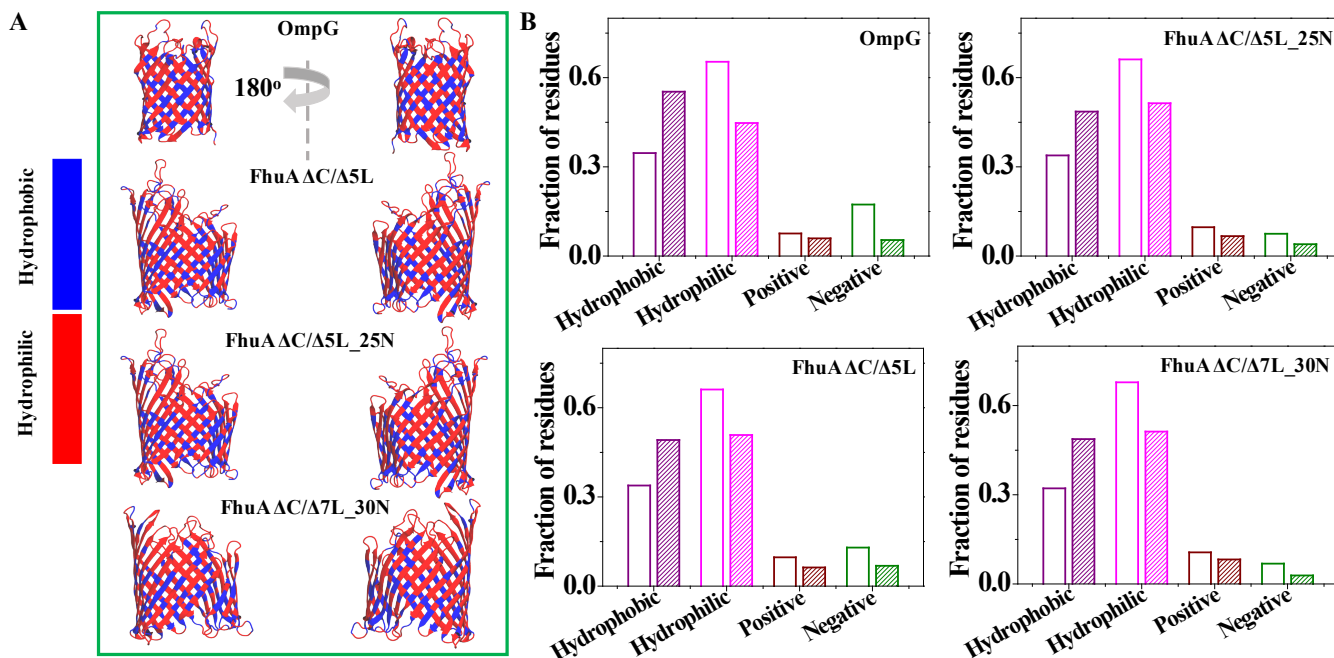


Figure S8: DDM binding versus residue type. (A) Molecular structures of the four β -barrel proteins colored to highlight the presence of the hydrophobic (blue) and hydrophilic (red) residues. The proteins are shown from the same viewpoints as in Fig. 6E; (B) The fraction of the hydrophobic, hydrophilic (polar or charged), as well as positively and negatively charged residues in the respective protein structures (open bars) and the fraction of those residues that bind to DDM (filled bars) during the steady-state (last ~ 70 ns) parts of the MD trajectories. For each protein, the data were averaged over the two independent MD trajectories, which were different by the initial arrangement of the DDM molecules. The hydrophobic residues of OmpG bind DDM 60% more likely than suggested by their abundance in the structure, whereas the hydrophobic residues of FhuA variants bind DDM 47% more likely than suggested by the structure.

Table S5: Biophysical properties of the α -helical proteins used in this study.⁶⁻⁷

Protein	pI	GRAVY ¹	Aliphatic index ²	Negative residues	Positive residues	Total number of residues
SELENOK U92C	10.34	-0.723	59.22	8	15	102
SELENOS U188S	9.72	-0.791	70.89	24	34	190

¹The GRAVY hydrophobicity parameter was calculated by adding individual hydropathy indexes⁸ of each residue and dividing by the total number of the protein residues. Increasing positive GRAVY number shows a more hydrophobic protein.

²The aliphatic index is given by the relative volume of aliphatic chain-containing residues.⁹

Table S6: Table that summarizes the recorded minima and maxima of the anisotropy readout with the SELENOK U92C and SELENOS U188S α -helical membrane proteins solubilized in DDM.^a This table also illustrates the rotational diffusion coefficients as well as alterations in the hydrodynamic radii of the proteomicelles during the two-state detergent desolvation transitions.

Protein ^b	r_{\min}^c	r_{\max}^c	$D_r^{\text{slow}} (10^9 \text{ s}^{-1})^d$	$D_r^{\text{fast}} (10^9 \text{ s}^{-1})^d$	$R_h^{\max} (\text{nm})^e$	$\Delta R_h (\text{nm})^f$
SELENOK U92C	0.095 ± 0.002	0.283 ± 0.023	0.016 ± 0.004	0.127 ± 0.003	2.1	1.1 ± 0.2
SELENOS U188S	0.103 ± 0.002	0.282 ± 0.029	0.017 ± 0.005	0.114 ± 0.003	2.1	1.0 ± 0.2

^aTo reach low detergent concentrations below the CMC, the Gdm-HCl-solubilized protein was refolded at detergent concentrations above the CMC.

^bDetails about these proteins are provided in **Methods**.

^cExperimentally determined anisotropy minima (r_{\min}) and maxima (r_{\max}). r_{\min} was extrapolated for the lowest detergent concentration in the well. r_{\max} was determined for detergent concentrations above the CMC.

^d D_r^{slow} and D_r^{fast} indicate the rotational diffusion coefficients of the proteins under solvation and desolvation conditions, respectively.

^e R_h^{\max} are the maximum hydrodynamic radii of the proteomicelle with various solubilizing detergents.

^f ΔR_h is the decrease in the hydrodynamic radius, R_h , as a result of the detergent desolvation transition.

Table S7: Summary of the fitting results of the two-state, concentration-dependent anisotropy curves acquired with SELENOK U92C and SELENOS U188S α -helical transmembrane proteins. DDM was the detergent used in this case. The protein concentration in the well was 200 nM. The initial detergent concentration was 1.3 mM. The FP measurements were carried out using a solution that contained 200 mM NaCl, 50 mM HEPES, pH 7.4 at a temperature of 24°C. All data were derived as averages \pm SDs of three independent data acquisitions.

Protein	p^b	K_d^c (mM)	q^d (mM ⁻¹)	ΔG^e (kcal/mol)	Balance ^f
SELENOK U92C	3.1 ± 1.6	0.29 ± 0.13	0.50	-4.8 ± 0.3	$F_{\text{adh}} \leq F_{\text{coh}}$
SELENOS U188S	4.8 ± 5.0	0.55 ± 0.12	0.39	-4.4 ± 0.1	$F_{\text{adh}} < F_{\text{coh}}$

^aExperimentally determined anisotropy minima (r_{\min}) and maxima (r_{\max}) for various detergents and proteins. r_{\min} was extrapolated for the lowest detergent concentration in the well. r_{\max} was determined for detergent concentrations above the CMC.

^b p is the Hill coefficient

^cThe apparent dissociation constant, K_d , was determined as the midpoint of the dose-dependent dissociation phase (e.g., c_0).⁵

^dThe slope factor or transition steepness was calculated at the midpoint of the dissociation phase.

^eFree energies were determined using the standard thermodynamic relationship $\Delta G = RT \ln K_d$.

^fThe quantitative balance between the adhesive protein-detergent (F_{adh}) and cohesive detergent-detergent interactions (F_{coh}) of the proteomicelles.

REFERENCES

1. Gradinaru, C. C.; Marushchak, D. O.; Samim, M.; Krull, U. J., Fluorescence anisotropy: from single molecules to live cells. *Analyst* **2010**, *135* (3), 452-9.
2. Prazeres, T. J. V.; Fedorov, A.; Barbosa, S. P.; Martinho, J. M. G.; Berberan-Santos, M. N., Accurate determination of the limiting anisotropy of rhodamine 101. Implications for its use as a fluorescence polarization standard. *J. Phys. Chem. A* **2008**, *112* (23), 5034-5039.
3. Lakowicz, J. R., *Principles of fluorescence microscopy*. 2nd ed.; Springer: New York, 2006.
4. Lide, D. R. E., *CRC Handbook of chemistry and physics - A ready reference book of chemical and physical data*. The 88th ed.; CRC Press - Taylor and Francis Group: Boca Raton 2008.
5. Rossi, A. M.; Taylor, C. W., Analysis of protein-ligand interactions by fluorescence polarization. *Nat. Protoc.* **2011**, *6* (3), 365-87.
6. Gasteiger, E.; Gattiker, A.; Hoogland, C.; Ivanyi, I.; Appel, R. D.; Bairoch, A., ExPASy: The proteomics server for in-depth protein knowledge and analysis. *Nucleic Acids Res.* **2003**, *31* (13), 3784-3788.
7. Gasteiger, E.; Hoogland, C.; Gattiker, A.; Duvaud, S.; Wilkins, M. R.; Appel, R. D.; Bairoch, A., Protein identification and analysis tools on the ExPASy server. In *Proteomics Protocols Handbook*, J.M., W., Ed. Humana Press: 2005; pp 571-607.
8. Kyte, J.; Doolittle, R. F., A simple method for displaying the hydropathic character of a protein. *J. Mol. Biol* **1982**, *157* (1), 105-132.
9. Ikai, A., Thermostability and aliphatic index of globular proteins. *J. Biochem.* **1980**, *88* (6), 1895-1898.